

Quantum computing with complex instruction sets

G. D. Sanders, K. W. Kim, and W. C. Holton

Department of Electrical and Computer Engineering, North Carolina State University, Raleigh, North Carolina 27695-7911

(Received 7 July 1998)

In most current quantum computers simple electromagnetic pulses implement computations using a minimal set of universal gates. We propose an approach in which quantum control techniques combined with flexible electromagnetic pulse shaping are used to replace *several* universal gates with a *single* instruction. We show that this complex instruction set approach can significantly reduce the time required to perform quantum computations. [S1050-2947(99)08902-7]

PACS number(s): 03.67.Lx, 89.80.+h

Quantum computers have attracted much interest since quantum theory allows parallelism in ways that are not possible with classical computers [1–3]. The earliest quantum algorithm that demonstrated an advantage of quantum algorithms over classical ones is the Deutsch-Josza algorithm [4]. As refined by Cleve *et al.* [5], it determines whether a function mapping N bits to one bit is constant or balanced with a single function call independent of the input size N , as opposed to $2^{N-1} + 1$ function calls required on a classical computer. Other efficient quantum algorithms have been found including Shor's algorithm for factoring integers [6] and Grover's algorithm for searching a database [7].

Several quantum computer architectures have been proposed. Cirac and Zoller proposed a quantum computer architecture based on laser-cooled trapped atomic ions [8] and Monroe *et al.* [9] demonstrated a CONTROLLED NOT gate in a 2-quantum-bit (qubit) trapped ion computer. Other architectures have been proposed based on cavity quantum electrodynamics [10], quantum dots [11], and solution nuclear magnetic resonance (NMR) [12]. In the NMR approach, the Deutsch-Josza [13,14] and Grover algorithms [15] have been demonstrated on 2-qubit computers. A NMR quantum computer has also been used to demonstrate 3-qubit error correction [16]. In these architectures, *electromagnetic pulses are used to implement quantum logic gates*. Quantum logic gates are unitary operators applied to qubit wave functions and depend on the Hamiltonian of the quantum computer and its interaction with the electromagnetic pulse. A universal quantum computer can be created using a set of universal gates and applying these gates sequentially [17,18]. By analogy with classical computers, we refer to this as *reduced instruction set quantum computing* (RISC QC). Decoherence of the quantum computer limits the number of instructions that can be executed in the serial RISC approach.

In this paper we consider an alternative to RISC QC. Regardless of the number of steps used in a computation, the unitary matrix of the overall computation is a matrix of the same size as those used in RISC gates. This suggests that we might replace a RISC sequence with a single complex instruction having an optimally tailored electromagnetic pulse. We refer to this approach as *complex instruction set quantum computing* (CISC QC). In CISC QC, *one trades the requirement for long coherence times for the ability to design and generate a more complex pulse shape*.

Designing pulse shapes to achieve a desired goal in a quantum system is the subject of quantum control theory.

Judson and Rabitz [19] have proposed teaching lasers to control femtochemistry experiments using a feedback loop. In their scheme, a laser pulse is found which maximizes a desired experimental outcome. A *theoretical* connection between quantum computing and quantum control has been established by Ramakrishna and Rabitz [20]. They show that universality of any quantum computing element is related to the controllability of a quantum control system.

Our focus is to investigate whether quantum control can be applied to the design of pulses for CISC QC. In *ideal* quantum computers, information is stored in a Hilbert space \mathcal{H} , which is a tensor product of Hilbert spaces of distinguishable two-state systems. The total Hilbert space is

$$\mathcal{H} = \mathcal{H}_0 \otimes \mathcal{H}_1 \otimes \cdots \otimes \mathcal{H}_{N-1}, \quad (1)$$

where \mathcal{H}_i is the Hilbert space of the i th two-state system. A state of \mathcal{H}_i is a qubit and information is stored in a state of \mathcal{H} . The binary string $S = s_0 s_1 \cdots s_{N-1}$, ($s_i = 0, 1$) can be encoded in the state

$$|S\rangle = |s_0, s_1, \dots, s_{N-1}\rangle = |s_0\rangle |s_1\rangle \cdots |s_{N-1}\rangle. \quad (2)$$

In quantum computation, a unitary operator determines the evolution of a wave function. A quantum computer carries out a computation through application of a controlled sequence of unitary matrices (gates) which act on qubits. The wave function $|\psi(t)\rangle$ is related to the evolution operator $U(t)$ and the initial wave function $|\psi(0)\rangle$ by $|\psi(t)\rangle = U(t)|\psi(0)\rangle$. The gate equation is

$$i\hbar \frac{\partial U(t)}{\partial t} = H(t)U(t), \quad (3)$$

which is subject to initial condition $U(0) = I$ and target condition $U(T) = U^0$. In Eq. (3), I is the identity matrix and U^0 is the matrix of the desired gate.

To proceed further, we must specify the Hamiltonian. While the Hamiltonian depends on the computer architecture, we suspect our overall conclusions will be independent of the Hamiltonian chosen. In a study of quantum logic gates, Barenco *et al.* [11] proposed an implementation of a 2-qubit CONTROLLED NOT gate based on optically driven quantum dots coupled by dipole-dipole interactions. The system can be modeled by a Hamiltonian [11]:

$$H(t) = \begin{pmatrix} \frac{-\Delta E_1 - \Delta E_2 - \hbar C_R}{2} & -\mu_2 E(t) & -\mu_1 E(t) & 0 \\ -\mu_2 E(t) & \frac{-\Delta E_1 + \Delta E_2 + \hbar C_R}{2} & 0 & -\mu_1 E(t) \\ -\mu_1 E(t) & 0 & \frac{+\Delta E_1 - \Delta E_2 + \hbar C_R}{2} & -\mu_2 E(t) \\ 0 & -\mu_1 E(t) & -\mu_2 E(t) & \frac{+\Delta E_1 + \Delta E_2 - \hbar C_R}{2} \end{pmatrix} \begin{matrix} |0,0\rangle \\ |0,1\rangle \\ |1,0\rangle \\ |1,1\rangle \end{matrix}, \quad (4)$$

where basis states in \mathcal{H} are indicated for clarity. The parameters ΔE_i and μ_i represent the energy gap and dipole matrix element between states $|0\rangle$ and $|1\rangle$ in the i th qubit, $\hbar C_R$ is the dipole-dipole coupling energy, and $E(t)$ is the optical field used to execute quantum computations. We adopt this as a model system and take $\Delta E_1 = 80$ meV, $\Delta E_2 = 110$ meV, $\mu_1 = \mu_2 = 100$ Å, and $\hbar C_R = 10$ meV. We can easily construct an energy diagram for \mathcal{H} . Denoting the energies of our states as E_{ij} , we have $E_{0,0} = -100$ meV, $E_{1,0} = -10$ meV, $E_{0,1} = 20$ meV, and $E_{1,1} = 90$ meV.

The quantum control problem of finding an optimal pulse shape is solved using a variational approach. We assume $E(t)$ can be described by a chirped Gaussian pulse

$$E(t) = E_0 \exp\left[-\left(\frac{t-t_0}{\Gamma}\right)^2\right] \cos[\Theta(t)]. \quad (5)$$

The field $E(t)$ is a carrier wave with time-dependent phase $\Theta(t)$ modulated by a Gaussian envelope with an amplitude E_0 peaked at time t_0 and having width Γ . The phase $\Theta(t)$ is expanded in a Taylor series in $t-t_0$ and terms through fourth order retained. Thus, following Ref. [21],

$$\Theta(t) = \theta_0 + \frac{\hbar\omega}{1!} \left(\frac{t-t_0}{\hbar}\right) + \frac{\alpha^2}{2!} \left(\frac{t-t_0}{\hbar}\right)^2 + \frac{\beta^3}{3!} \left(\frac{t-t_0}{\hbar}\right)^3 + \frac{\gamma^4}{4!} \left(\frac{t-t_0}{\hbar}\right)^4, \quad (6)$$

where θ_0 is the phase constant, $\hbar\omega$ is the center energy, and α , β , and γ are linear, quadratic, and cubic chirp energies.

To see how well a given pulse performs, we define a fitness function χ [a nonlinear function of the parameters describing $E(t)$] as

$$\chi = \left(\frac{1}{N_U} \sum_{i,j} \left| U_{i,j}(T) - U_{i,j}^0 \right|^2 \right)^{1/2}. \quad (7)$$

In Eq. (7), $U_{i,j}^0$ is the unitary matrix for the target gate, $N_U = 16$ is the number of elements in $U(t)$, and χ is a measure of the average root mean squared error per matrix element. An acceptable pulse shape is found when χ falls below an error threshold of 5×10^{-3} . To find optimal pulse parameters, we minimize χ using a genetic optimization routine.

As an example, we consider a 2-qubit EXCHANGE gate which can be implemented by three CONTROLLED NOT gates CNOT12, CNOT21, and CNOT12, applied in sequence. Here the first integer specifies the control bit, which remains unchanged, and the second integer specifies the target bit, which flips only if the control bit is set to 1.

The operation of a CONTROLLED NOT gate acting on the product state in \mathcal{H} encoding control qubit i and target qubit j is defined as

$$U_{\text{CNOT}}^{ij} |c\rangle_i |t\rangle_j = |c\rangle_i |t \oplus c\rangle_j, \quad (8)$$

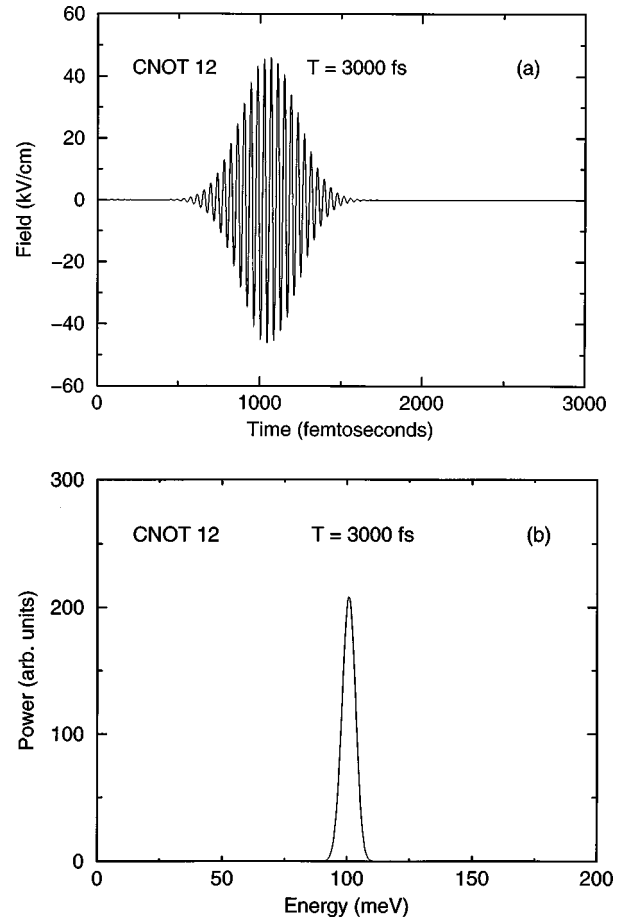


FIG. 1. Optimal pulse for CNOT21 gate in a model 2-qubit quantum computer determined by a genetic algorithm. The pulse profile is shown in (a) and the power spectrum is shown in (b).

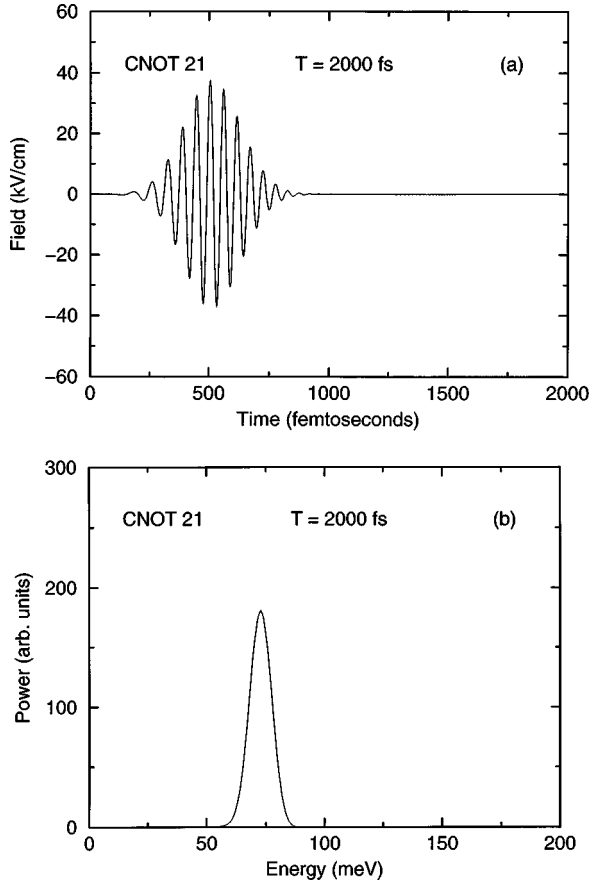


FIG. 2. Optimal pulse for CNOT12 gate in a model 2-qubit quantum computer determined by a genetic algorithm. The pulse profile is shown in (a) and the power spectrum is shown in (b).

where $t \oplus c$ is the EXCLUSIVE OR of t and c . The two CONTROLLED NOT operators in a 2-qubit quantum computer are unitary matrices in \mathcal{H} denoted CNOT12 and CNOT21. It follows from Eq. (8) that CNOT12 can be implemented through an optical transition between states $|1,0\rangle$ and $|1,1\rangle$, while CNOT21 can be implemented via an optical transition between $|0,1\rangle$ and $|1,1\rangle$. From the energy level diagram for \mathcal{H} , we find that the transition energy for CNOT12 is $\hbar\omega_{\text{CNOT12}}=100$ meV while for CNOT21, $\hbar\omega_{\text{CNOT21}}=70$ meV.

The EXCHANGE gate is defined by

$$U_{\text{EXCHANGE}}^{ij}|a\rangle_i|b\rangle_j=|b\rangle_i|a\rangle_j \quad (9)$$

and the unitary matrix for the EXCHANGE operator can be written down from the definition or obtained by carrying out a multiplication of CONTROLLED NOT matrices:

$$U_{\text{EXCHANGE}}^{12}=U_{\text{CNOT}}^{12}U_{\text{CNOT}}^{21}U_{\text{CNOT}}^{12}. \quad (10)$$

Equations (9) and (10) suggest two possible implementations of the EXCHANGE gate, i.e., RISC and CISC. In the RISC approach, the CONTROLLED NOT gates are performed sequentially as indicated in Eq. (10) by applying three Gaussian pulses with central energies of $\hbar\omega=100$, 70, and 100 meV, respectively. At the same time, we see from Eq. (9)

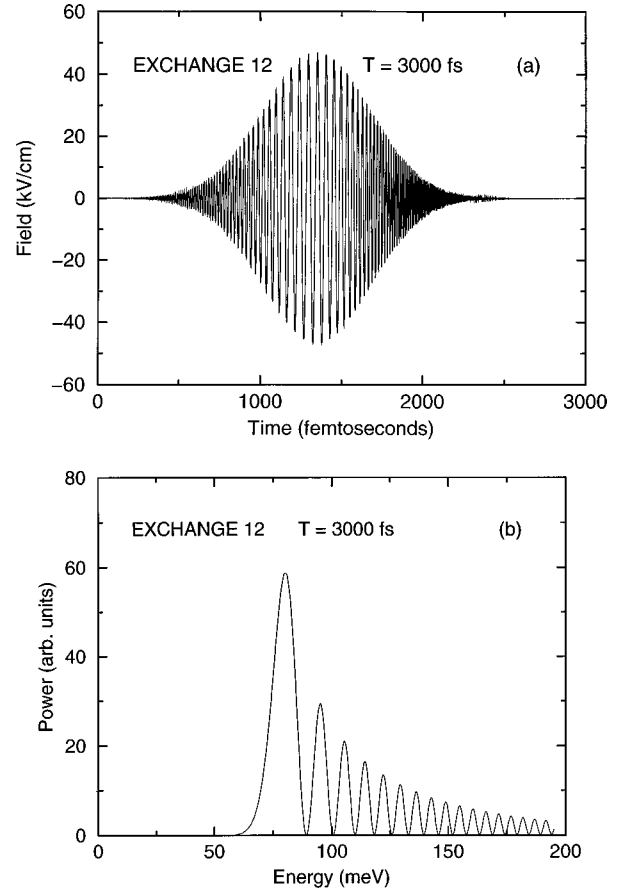


FIG. 3. Optimal pulse for EXCHANGE gate in a model 2-qubit quantum computer determined by a genetic algorithm. The pulse profile is shown in (a) and the power spectrum is shown in (b).

that the EXCHANGE gate may also be obtained directly by an optical transition between $|1,0\rangle$ and $|0,1\rangle$ at an energy of $\hbar\omega_{\text{EXCHANGE}}=30$ meV.

To illustrate the RISC approach, the gate equations for the CONTROLLED NOT gates are solved numerically. We set the target time $T=2500$ fs and use the genetic algorithm to evolve an optimal pulse shape. The results for CNOT21 are shown in Fig. 1 where we plot the optimal field $E(t)$ and its power spectrum $E(\hbar\omega)$. As seen in Fig. 1, the system implements CNOT21 with a simple Gaussian pulse with essentially no chirp. As expected, the power spectrum shows a peak near $\hbar\omega_{\text{CNOT21}}=70$ meV. The results for CNOT12 are shown in Fig. 2 where the optimal field and its power spectrum are plotted. We chose our target time to be $T=3000$ fs. In this case, we obtain a narrow peak in the power spectrum centered at the CNOT12 transition energy $\hbar\omega_{\text{CNOT12}}=100$ meV. Again, there is virtually no chirp present in the optimal pulse. We thus find we can implement the EXCHANGE gate by applying three Gaussian pulses in sequence for a total computation time of $T_{\text{RISC}}=8500$ fs. The choice of target times for the CONTROLLED NOT gates was *not* arbitrary. The values we chose were the shortest we could use and still get nice monochromatic pulses and convergence of χ to within our specified tolerance. We did this to be faithful to the spirit of the RISC QC paradigm.

The EXCHANGE gate can also be implemented with a Gaussian pulse having a transition energy of 30 meV provided that T is large enough. But with the CISC paradigm we

can, in fact, do better. To illustrate the advantage of the CISC approach in implementing the EXCHANGE gate, we set the target time to $T=3000$ fs, i.e., we seek to perform the EXCHANGE gate in roughly $\frac{1}{3}$ the time required for the RISC implementation using only a single chirped Gaussian pulse. The results are shown in Fig. 3. Clearly, our results demonstrate that the CISC approach can achieve the desired computing operation in a considerably shorter time frame compared to the RISC treatment. We note that the power spectrum is not centered at the expected EXCHANGE transition energy of 30 meV. *The selected target time is simply too short for this to be workable.* Instead, the system evolves a complicated and highly nonintuitive chirped Gaussian pulse centered at higher energy. As seen in Fig. 3, the power spectrum for $E(t)$ has a sharp peak at 80 meV with fringes at higher energies. Interestingly, the large peak seen at 80 meV is roughly midway between the monochromatic transition energies for CNOT12 and CNOT21. As the desired target time is reduced, it is expected that the pulse shape would become more complex until an absolute minimum target time is reached.

To summarize, we can achieve the EXCHANGE gate in one of two ways. In the RISC approach, we apply three simple Gaussian pulses and achieve the desired result in 8500 fs. In the CISC approach, we apply a single chirped Gaussian pulse and achieve the same result in 3000 fs. Thus a reduction in computation time is achieved at the expense of

generating a more complicated (and nonintuitive) pulse shape. It is expected that the CISC paradigm can realize similar advantages over the RISC approach in other crucial quantum logic gates.

The pulse shapes presented here result from simulating a quantum computer on a classical one. Feedback from the simulated computer was used to obtain pulses that implement desired gates. Our simulations are limited to a few qubits since the time required to simulate a quantum computer grows exponentially with the number of qubits. In implementing CISC, feedback needs to come from the quantum computer, not a simulation thereof. Quantum control with feedback from a quantum computer offers a way to train the computer to perform gates. Error reduction is enhanced in this approach since the system finds the pulse shape that gives the highest experimental fidelity. Once the pulse is learned, it can be used whenever the gate is applied in a computation. We note that CISC does not eliminate the need for quantum error correction in long computations. However, it may make error correction more robust (i) by providing gates of *optimal fidelity* and (ii) by combining short sequences of RISC gates into *single* instructions and reducing the overall computation time.

This work was supported, in part, by the Defense Advanced Research Project Agency and the U.S. Office of Naval Research.

-
- [1] Seth Lloyd, *Sci. Am. (Int. Ed.)* **273**, 140 (1995).
 - [2] D. P. DiVincenzo, *Science* **270**, 255 (1995).
 - [3] A. Ekert and R. Josza, *Rev. Mod. Phys.* **68**, 733 (1996).
 - [4] D. Deutsch and R. Josza, *Proc. R. Soc. London, Ser. A* **439**, 553 (1992).
 - [5] R. Cleve, A. Ekert, C. Macchiavello, and M. Mosca, *Proc. R. Soc. London, Ser. A* **454**, 339 (1998).
 - [6] P. W. Shor, in *Proceedings of the 35th Annual Symposium on Foundations of Computer Science*, edited by S. Goldwasser (IEEE Computer Society Press, New York, 1994), pp. 124–134.
 - [7] L. K. Grover, *Phys. Rev. Lett.* **79**, 325 (1997).
 - [8] J. I. Cirac and P. Zoller, *Phys. Rev. Lett.* **74**, 4091 (1995).
 - [9] C. Monroe, D. M. Meekhof, B. E. King, W. M. Itano, and D. J. Wineland, *Phys. Rev. Lett.* **75**, 4714 (1995).
 - [10] T. Sleator and H. Weinfurter, *Phys. Rev. Lett.* **74**, 4087 (1995).
 - [11] A. Barenco, D. Deutsch, A. Ekert, and R. Josza, *Phys. Rev. Lett.* **74**, 4083 (1995).
 - [12] N. Gershenfeld and I. L. Chuang, *Science* **275**, 350 (1997).
 - [13] J. A. Jones, e-print quant-ph/9801027.
 - [14] I. L. Chuang, L. M. K. Vandersypen, X. Zhou, D. W. Leung, and Seth Lloyd, e-print quant-ph/9801037.
 - [15] I. L. Chuang, N. Gershenfeld, and M. Kubinec, *Phys. Rev. Lett.* **80**, 3408 (1998).
 - [16] D. G. Cory, W. Mass, M. Price, E. Knill, R. Laflamme, W. H. Zurek, T. F. Havel, and S. S. Somaroo, e-print quant-ph/9802081.
 - [17] S. Lloyd, *Phys. Rev. Lett.* **75**, 346 (1995).
 - [18] D. P. DiVincenzo, *Phys. Rev. A* **51**, 1015 (1995).
 - [19] R. S. Judson and H. Rabitz, *Phys. Rev. Lett.* **68**, 1500 (1992).
 - [20] V. Ramakrishna and H. Rabitz, *Phys. Rev. A* **54**, 1715 (1996).
 - [21] J. L. Krause, D. H. Reitze, G. D. Sanders, A. V. Kuznetsov, and C. J. Stanton, *Phys. Rev. B* **57**, 9024 (1998).